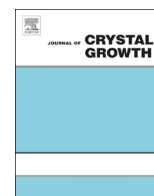




ELSEVIER

Contents lists available at SciVerse ScienceDirect

## Journal of Crystal Growth

journal homepage: [www.elsevier.com/locate/jcrysgr](http://www.elsevier.com/locate/jcrysgr)

# Growth mechanism of CuZnInSe<sub>2</sub> thin films grown by molecular beam epitaxy



Ya Hsin Tseng<sup>a,b</sup>, Chu Shou Yang<sup>a,\*</sup>, Chia Hsing Wu<sup>a</sup>, Jai Wei Chiu<sup>a</sup>, Min De Yang<sup>c</sup>, Chih-Hung Wu<sup>c</sup>

<sup>a</sup> Graduate Institute of Electro-optical Engineering, Tatung University, Taipei, Taiwan

<sup>b</sup> Department of Electro-physics, National Chiao-Tung University, Hsin-Chu, Taiwan

<sup>c</sup> Institute of Nuclear Energy Research, P.O. Box 3-11, Lungtan 32500, Taiwan

## ARTICLE INFO

Available online 4 January 2013

Keywords:

A1. X-ray diffraction

A3. Molecular beam epitaxy

B1. CuZnInSe<sub>2</sub>

B2. Semiconductor materials

## ABSTRACT

CuZnInSe<sub>2</sub> (CZIS) has potential application in solar cell for absorption layer, and give an advantage to change the band gap from CuInSe<sub>2</sub> (1.02 eV) to ZnSe (2.67 eV). Using molecular beam epitaxy technology, the CZIS thin films were grown via CuInSe (CIS) and ZnSe base. In the case of CIS, thin films were grown on Mo-coated soda lime glass with various zinc flux. CIS was transformed into chalcopyrite and sphalerite coexisting CZIS easily but it is difficult to transform into the pure sphalerite CZIS. Zn/(Zn + In + Cu) ratio has limited to approximate 36 at% and the excess-Zn played a catalyst role. In the case of ZnSe base, which was grown on GaAs (001), various In and Cu flux defined as the  $T_{In}$  series and  $T_{Cu}$  series, respectively. There are four types of compound in the  $T_{In}$  series and  $T_{Cu}$  series, including ZnSe, In<sub>x</sub>Se<sub>y</sub>, ZnIn<sub>2</sub>Se<sub>4</sub> (ZIS) and CZIS. In the  $T_{In}$  series under the lowest In and Cu flux, selenium (Se) were randomly combined with cations to form the CZIS. When  $T_{In}$  is increased in this moment, the CZIS was transformed into ZIS. In the  $T_{Cu}$  series, CZIS demonstrated via In-rich ZIS (Zn(In, Cu)Se) and In<sub>x</sub>Se<sub>y</sub> base ((Zn, Cu)InSe). It is chalcopyrite and sphalerite coexisting structure in the medium  $T_{Cu}$  region. In the high  $T_{Cu}$  region, it is transformed into the Zn-poor and Cu-rich CZIS.

© 2012 Elsevier B.V. All rights reserved.

## 1. Introduction

The quaternary compounds, I–II–III–VI<sub>2</sub> group, have high absorption coefficient about  $10^4$ – $10^5$  cm<sup>-1</sup> within widely absorption range from visible to near infra-red region, outdoor stability and a significant resistance to radiation damage [1]. CuZnInSe (CZIS) is one of the potential materials for absorber layer in solar cell applications. The consisted within I–II–III–VI<sub>2</sub> group elements is defined by (CuInSe<sub>2</sub>)<sub>1-x</sub>-(2ZnSe)<sub>x</sub> solid solution [1–3]. It has binary structures, chalcopyrite and sphalerite (zinc blende like), which were associated with the Zn content [4]. The chalcopyrite structure resembles CIS, with the Cu and In sites randomly substituted by Zn atoms. The sphalerite structure is like ZnSe, with the position of metal sub-lattice occupied statistically by Cu, In and Zn atoms.

A number of methods for growing CuZnInSe absorber layers have been reported so far. These methods include Bridgman growth [5], chemical vapor transport [5], two-stage technological process: standard thermal evaporation and selenization [6], radio frequency (RF)-sputter [7], pulsed laser deposition (PLD) [7] and

dc sputter [5]. Gremenok et al. [2,4] established the transition region from chalcopyrite structure to the sphalerite structure. The performance of CZIS solar cell linearly depends on composition. The highest solar efficiency was achieved to 7.2%. In order to further improve the conversion efficiency, it is important to understand the detail growth mechanism of CZIS. In this study, CZIS thin films were demonstrated using molecular beam epitaxy (MBE) via the precursor of CuInSe<sub>2</sub> (CIS) and ZnSe to understand the growth mechanism. The physical properties of CZIS are characterised by using X-ray diffraction, Raman scattering, and EDX measurements.

## 2. Experiments

The CZIS thin films were demonstrated via the precursor of CuInSe<sub>2</sub> (CIS) and ZnSe with varied K-cell temperature of Zn, In, and Cu, which are denoted as  $T_{Zn}$ ,  $T_{In}$ ,  $T_{Cu}$  series. The growth parameters of CZIS thin films are listed in Table 1. In samples-1–5, i.e.  $T_{Zn}$  series, the CZIS thin films were deposited on Mo-coated soda lime glass. The growth condition is based on chalcopyrite CIS with supplied zinc source, which varied  $T_{Zn}$  from 300 to 340 °C. On the contrary, the  $T_{In}$  series were based on ZnSe with turning

\* Corresponding author. Tel.: +886 2 21822928x6612.  
E-mail address: [csyang@ttu.edu.tw](mailto:csyang@ttu.edu.tw) (C.S. Yang).

**Table 1**  
Growth parameters of CuZnInSe<sub>2</sub> compounds in  $T_{Zn}$ ,  $T_{In}$ , and  $T_{Cu}$  series.

Sample number	Sample	Substrate (°C)	Selenium (°C)	Zinc (°C)	Indium (°C)	Copper (°C)	Zn/(Zn+Cu+In) (at%)	Cu/(Zn+Cu+In) (at%)	In/(Zn+Cu+In) (at%)
1	CuInSe $T_{Zn}$ series	500	203		655	1150			
2		550	203	<b>300</b>	655	1150	20.4	53.3	26.2
3				<b>310</b>			28.8	56.7	14.4
4				<b>320</b>			35.6	48.4	15.8
5				<b>330</b>			36.1	48.6	15.3
6	ZnSe $T_{In}$ series	300	198	315					
7		500	198	315	<b>575</b>	1000	52.4	18.9	28.7
8					<b>585</b>		36.9	38.7	24.4
9					<b>600</b>		61.5	21.9	16.6
10					<b>615</b>		38.3	16.5	45.2
11	$T_{Cu}$ series	500	198	315	630	<b>1012</b>	33.9	24.7	41.4
12						<b>1025</b>	38.8	22.9	38.3
13						<b>1037</b>	39.6	26.6	33.8
14						<b>1050</b>	32.2	27.4	40.4
15						<b>1062</b>	42.6	34.2	23.2
16						<b>1075</b>	9.8	59.6	30.6
17						<b>1087</b>	10.7	61.7	27.6
18						<b>1100</b>	8.5	62.3	29.2

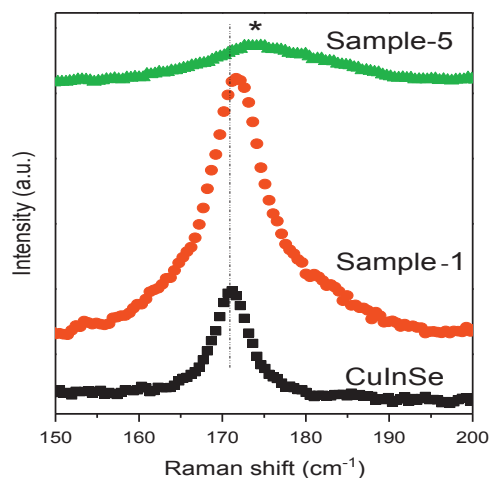


**Fig. 1.** Raman scattering spectra of CuInSe<sub>2</sub> and CuZnInSe<sub>2</sub> of samples-1 and 5.

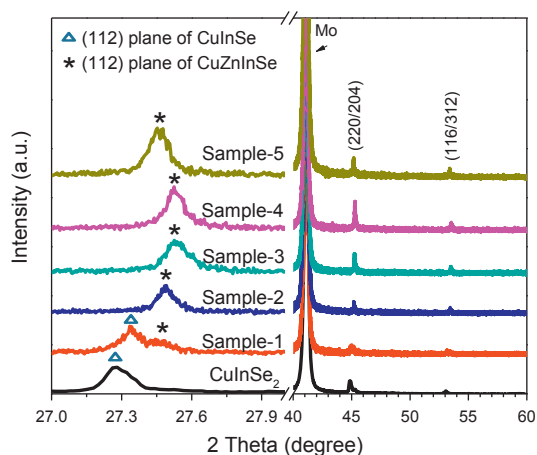


**Fig. 2.** XRD patterns of CuZnInSe<sub>2</sub> in  $T_{Zn}$  series.

the  $T_{In}$  from 575 to 645 °C. In  $T_{Cu}$  series, these sample parameters are similar to sample-10. The variable factor is the  $T_{Cu}$ . The thicknesses of samples-1–4 are around 300 nm, which were

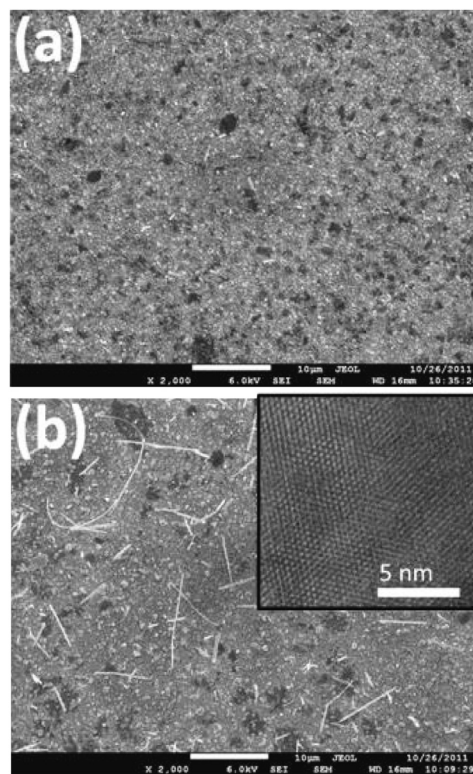


**Fig. 3.** Top view and cross-sectional SEM images of CuZnInSe<sub>2</sub> thin film with  $T_{Zn}$ =(a) 330 °C (sample-4) and (b) 340 °C (sample-5). The inset is a bright field high-resolution transmission electron microscopy image of CZIS wire, taken from sample-5.

determined by cross-sectional scanning electronic microscopy images. The growth rate of samples-1–4 is 1.25 nm/min, which is independent to the varying degree of zinc flux until the  $T_{Zn}$  reached 340 °C. In sample-5, the growth rate is dropped to 0.88 nm/min. The reason of decreasing growth rate is discussed latter. For  $T_{In}$  and  $T_{Cu}$  series, the growth rate is around 0.9 nm/min. The cation atomic ratio is calculated by the element atomic percentage, which is determined by energy dispersive spectrum. Raman scattering spectroscopy was excited by 514.5 nm-Ar ionic

laser and analyzed by a JY-550 spectrometer with the spectrum resolution of about 0.05 nm. The slit width was set at 100  $\mu\text{m}$ , and grating with 2400 grooves/mm was used. The structure analysis was performed using a D2 PHASER X-ray diffract meter employing  $\text{Cu}_{K\alpha}$  radiation with a wavelength of 1.5419  $\text{\AA}$ .

### 3. Results and discussions

#### 3.1. $T_{\text{Zn}}$ series: $\text{CuInSe}_2$ incorporated with varied content of Zn

Fig. 1 shows the Raman spectra of  $\text{CuInSe}_2$  and  $\text{CuZnInSe}$ , which is grown at  $T_{\text{Zn}}=300^\circ\text{C}$  (sample-1) and  $340^\circ\text{C}$  (sample-5). The CIS  $A_1$  phonon mode is slightly shifted to high frequency when zinc atom incorporated into CIS. It refers to the heavy atoms of indium ( $M=114.82$ ) that have replaced by slight atoms of zinc ( $M=65.38$ ). Additionally, when Cu–Se bonding was replaced by Zn–Se, the phonon frequency shifts toward high frequency has been mentioned [6]. It implies that the Zn–Se bonding was produced in the  $\text{CuInSe}_2$  crystal. XRD spectra of CZIS samples-1–5 and a reference sample of CIS are shown in Fig. 2. The XRD peaks

are associated to CZIS and CIS (112), (220/204), and (116/312), respectively. CIS and CZIS compounds are co-existed in sample-1 ( $T_{\text{Zn}}=300^\circ\text{C}$ ). Further increasing  $T_{\text{Zn}}$ , the crystal structure transforms to CZIS completely and the diffraction angle shifts to larger degree. According to the Raman and XRD spectra, the crystal structure of CZIS in  $T_{\text{Zn}}$  series is assumed to be chalcopyrite and sphalerite mixed. When  $T_{\text{Zn}}=340^\circ\text{C}$  (sample-5), the XRD peak shifts to inverse direction. This behavior is understood by the varied cation ratio. The cation ratio of  $\text{Zn}/(\text{Zn}+\text{Cu}+\text{In})$  is increased with  $T_{\text{Zn}}$  raised until  $T_{\text{Zn}}=330^\circ\text{C}$ , as shown in Table 1.

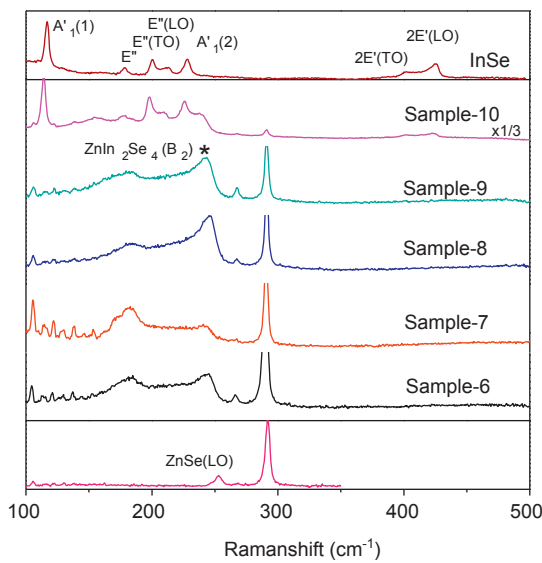


Fig. 4. Raman spectra of CZIS thin films in  $T_{\text{In}}$  series. Raman spectra of ZnSe and InSe are used for reference.

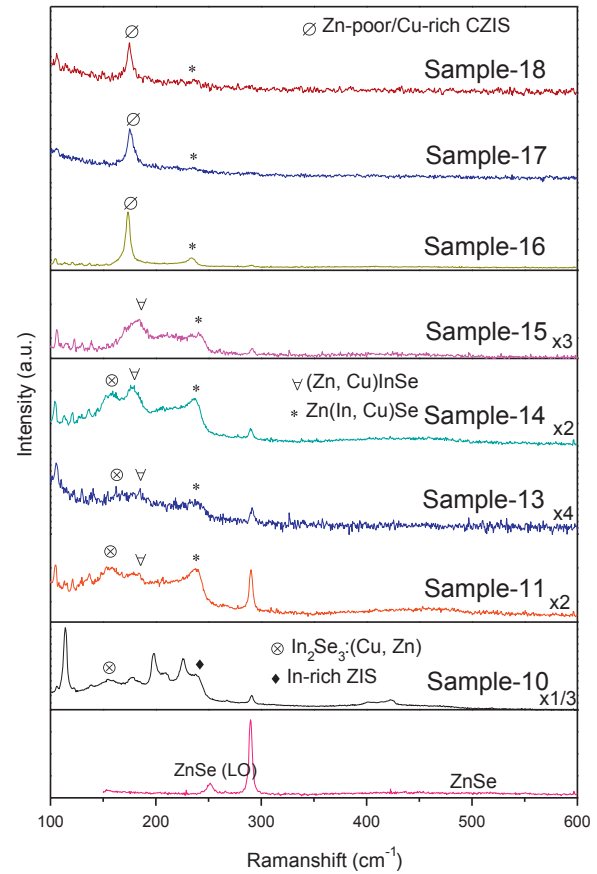


Fig. 6. Raman spectra of CZIS thin films in  $T_{\text{Cu}}$  series and a reference sample of ZnSe.

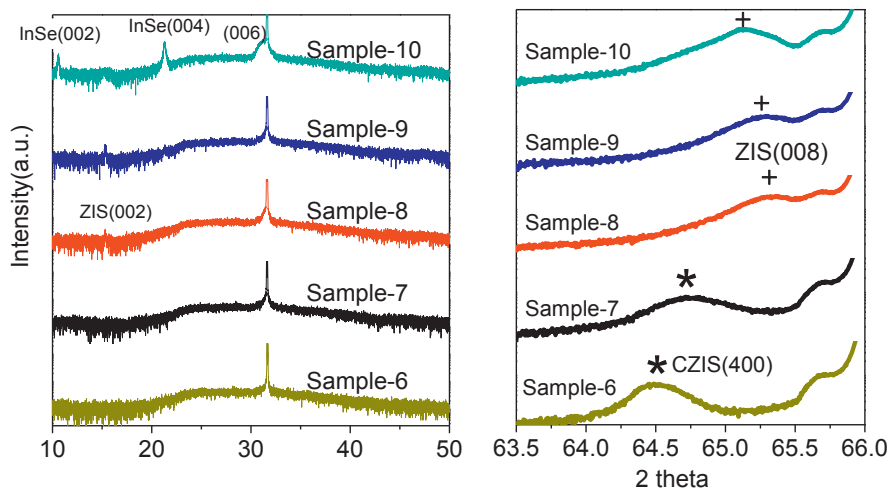


Fig. 5. XRD patterns of  $\text{CuZnInSe}$  in  $T_{\text{In}}$  series.

Further raising the  $T_{Zn}$  to 340 °C,  $Zn/(Zn+Cu+In)$  is declined. It implies that the excess-Zn played another role instead of transforming into purity sphalerite structure. Fig. 3(a) and (b) displays the top view SEM images of samples-4 and 5, respectively. Sample-5 has been observed as a dense nanowire on the surface. We assumed that the excess-Zn plays a catalyst role in the excess-Zn condition. A bright field transmission electron microscopy image of a wire, which took from sample-5, is shown in the inset of Fig. 3(b). The lattice constant is determined around 0.408 nm, which is similar to the XRD result (0.409 nm). It implies that wire is CZIS crystal, which is an identical case with thin film.

### 3.2. $T_{In}$ and $T_{Cu}$ series: ZnSe incorporated with varied content of Cu and In

Fig. 4 shows the Raman scattering spectra of  $T_{In}$  series samples, ZnSe,  $In_2Se_3$ , and InSe. These spectra are strongly correlated to the material content ratio. In the poor indium and copper region, i.e. samples-6–8, the Raman scattering patterns are similar to ZnSe. The longitudinal optical phonon (LO) of ZnSe ( $251\text{ cm}^{-1}$ ) reveals red-shift when indium and copper are incorporated. It is consistent with the results of  $T_{Zn}$  series. When indium content is dominated in total cation atoms, like sample-9, the phonon energy at around  $242\text{ cm}^{-1}$  is associated to  $ZnIn_2Se_4$   $B_2$  mode [7]. When  $T_{In}$  was increased to 630 °C (sample-10), the vibration mode of InSe bonding was presented due to the indium cation content ratio increasing to 78.6%. This phase transformation process is also observed in the XRD patterns. Fig. 5 exhibits the XRD spectra of samples-6–10. XRD pattern of CZIS (400), which is marked by a star symbol, is observed in samples-6 and 7. The crystalline transfers to ZIS as indium content reached 45.6%. Additionally, the InSe (002), (004) and (006) planes were observed in sample-10. In  $T_{In}$  series, the crystalline of CZIS is attributed to sphalerite. When the indium cation content ratio is higher than 45%, the sphalerite CZIS transformed to tetragonal ZIS and even hexagonal  $In_xSe_y$ .

Because the excess-In limited the ratio of  $x$  in the  $(CIS)_{1-x}(2ZnSe)_x$  solid solution, the  $T_{In}$  was fixed at 630 °C in  $T_{Cu}$  series. The copper content ratio is increased with the increase in  $T_{Cu}$ . The Raman spectra of  $T_{Cu}$  series samples are shown in Fig. 6. According to Fig. 6, the  $T_{Cu}$  series samples were separated into four parts:

(1) In sample-10, this Raman spectrum includes the phonon modes of  $In_xSe_y$ : (Cu, Zn) and In-rich ZIS:Cu, which are symbolized by open circle and down-toward-triangle, respectively.

- (2) At  $T_{Cu}=1012\text{--}1050\text{ °C}$ , it includes  $Zn(In, Cu)Se$ , which means the In sites of In-rich ZIS were replaced by Cu, and  $(Zn, Cu)InSe$ , which means the Zn sites of  $In_xSe_y$ : (Zn, Cu) were replaced by Cu.
- (3) When  $T_{Cu}=1062\text{ °C}$ , the phonon mode of  $In_xSe_y$ : (Cu, Zn) disappeared.
- (4) When  $T_{Cu}$  exceeded 1075 °C, Zn-poor/Cu-rich CZIS was formed.

## 4. Conclusions

The crystal structure of  $CuZnInSe_2$  is controlled by turning the atomic content ratio. CZIS products have no purity sphalerite structure unless the excess Se-rich condition. In the CIS case, the Zn cation content ratio was limited at 37 at% due to the limited of cation/anion  $((Cu+In+Zn)/Se)$ . Further increasing the  $T_{Zn}$ , the Zn atom plays a role of catalyst to grow nanowire instead of inserting into the crystal structure. In the ZnSe case of  $T_{In}$  series, purity sphalerite CZIS structure was product in excess-Se-rich condition, and the  $T_{In}$  increasing leads to the transformation from sphalerite CZIS to tetragonal ZIS structure and even if the  $In_xSe_y$ . Furthermore, a pure chalcopyrite structure is exhibited in the copper-rich condition.

## Acknowledgment

This work was supported by the Nation Science Council under Grant number NSC-97-2112-M-036-002-MY3 and Tatung University under Grant number B100-O04-044.

## References

- [1] I.V. Bodnar, V.F. Gremenok, W. Schmitz, K. Bente, Th. Doering, *Crystal Research and Technology* 39 (4) (2004) 301–307.
- [2] V.F. Gremenok, E.P. Zaretskaya, V.M. Siarheyeva, K. Bente, W. Schmitz, V.B. Zaleski, H.J. Möller, *Thin Solid Films* 487 (2005) 193–198.
- [3] R.A. Wibowo, K.H. Kim, *Solar Energy Materials & Solar Cells* 93 (2009) 941–944.
- [4] V.F. Gremenok, W. Schmitz, I.V. Bodnar, K. Bente, Th. Doering, G. Kommichau, L.A. Victorov, A. Eifler, V. Riede, *Japanese Journal of Applied Physics* 39 (2000) 277–278.
- [5] V.A. Ivanov, V.F. Gremenok, V.M. Siarheyeva, E.P. Zaretskaya, V.B. Zaleski, V.I. Kovalevski, K. Bente, *Moldavian Journal of the Physical Sciences* 5 (N3–4) (2006) 355–359.
- [6] Y.H. Lin, Growth and characterization of  $Cu_xZn_{1-x}Se$  epilayers by MBE, Master theory, Graduate Institute of Electro-Optical Engineering, Tatung University, (2011) p. 37.
- [7] C. Razzetti, P.P. Lottici, S. Bini, M. Curti, *Physica Status Solidi B* 177 (1993) 525.